Slurry Bubble Column Dynamics

by

Dennis N. Smith, John A. Ruether, and Gary J. Stiegel

U.S. Department of Energy
Pittsburgh Energy Technology Center
P.O. Box 10940
Pittsburgh, Pennsylvania 15236
U.S.A.

ABSTRACT

A novel approach utilizing an electrical conductivity twin-probe technique is described for obtaining important gas-phase characteristics, such as bubble size, velocity, and holdup fraction. A 10-cm-internal-diameter by 310-cm-high glass column is employed to investigate the bubble dynamics measured with this probe. The liquid phase is composed of a mixture of ethanol and water that may have substantial "surface activity" that results in a dynamic surface tension effect on the rate of bubble coalescence. Measurements of gas holdup, bubble size, and velocity indicate the influence of surface activity on the gas phase characteristics. Possible implications of these results on the hydrodynamics of Fischer-Tropsch reactors are given.

Introduction

In the design of a slurry bubble column reactor for indirect liquefaction of coal, there has been considerable controversy over the transport phenomena associated with hydrodynamics, and mass and heat transfer [1-3]. This controversy is strongly related to the uncertainties in extrapolating transport coefficients obtained from cold model reactor data to a hot, pressurized reactor containing a mixture of synthesis gas, an inert liquid medium, catalyst, and low vapor pressure product waxes. Some important transport measurements, such as gas holdup and axial solids distributions,

have been measured (4) for a 2-inch-diameter by 25-foot-high slurry bubble column Fischer-Tropsch (F-T) reactor but have not been correlated by extension of cold model transport coefficient correlations. In addition, there exists a large uncertainty of scaling up the transport phenomena associated with a 2-inch-diameter reactor to a demonstration scale (1.5-meter-diameter) reactor.

A key parameter, bubble size distribution, must be known for F-T reactor design. The hydrodynamics of slurry bubble columns are very sensitive to this parameter, which, in turn, influences the mass and heat transfer. The bubble size distribution is a function of the initial bubble size generated from the distributor plate and the rate of coalescence and breakup of bubbles. For single component liquids, an equilibrium bubble size distribution is governed by the bulk liquid properties, such as density and viscosity, surface tension, the mixing intensity of the gas phase, and, in some instances, the initial bubble size generated from the distributor plate. For multicomponent liquid mixtures, the equilibrium bubble size is affected by the same phenomena as for single component liquids but additionally may be influenced by a dynamic surface tension effect.

It is the purpose of this work to demonstrate the effect of dynamic surface tension on the hydrodynamics of a slurry bubble column. Possible implications of these results on the hydrodynamics of a slurry phase Fischer-Tropsch reactor are given.

Experimental Apparatus

A 10-cm-diameter by 307-cm-long glass bubble column is employed in this investigation. The bubble column is sectionalized with alternating 30-cm lengths of glass pipe and 5-cm lengths of Teflon spacers. The Teflon spacers are employed as mounting devices for electrical conductivity probes and slurry sampling systems. A 15-cm-diameter expansion chamber is located at the top of the bubble column, achieving uniform gas disengagement. A ventilation hood is located above the expansion chambers to exhaust any vapors entrained in the gas phase. A 5-cm-diameter by 10-cm-diameter tee is located at the top of the bubble column, joining a 10-cm-diameter by 213-cm-long glass column that acts as an overflow/recirculation tank for the slurry. The gas phase is introduced through a 20-micron stainless steel sintered plate distributor at the bottom of the bubble columns. In addition to the above-mentioned 10-cm slurry bubble column apparatus, a 10.8-cm-diameter by 194-cm-long Plexiglass bubble column has been utilized to obtain gas holdup data with a 72 x 1-mm perforated plate distributor (5).

A depiction of a twin-electrode conductivity probe inserted into the slurry bubble column is given in Figure 1. The conductivity probe circuit and related data acquisition system are shown in Figure 2. The twin-electrode conductivity probe consists of two Teflon-coated wires with a diameter of 0.076 mm. The Teflon coating serves as a good moisture-repellent surface as well as an electrical insulator. Only the ends of the probe wires are exposed to obtain rapid response of the bubble-shedding water from the probe. A description of the data collection system for these conductivity probes has been given previously (6). Analysis of the signal

response considers two important signal characteristics, the dwell time of a bubble on each probe and the lag time associated with bubble traversing the gap between the two probes. The dwell time is obtained from the slopes of the signal response; the start of a bubble signal is indicated by exceeding a threshold slope, and the end of a bubble signal is when there is less than a threshold slope for two consecutive sampling intervals. The lag time between a pair of signals corresponding to the passage of a bubble is computed for the time interval during which the centroid of a pierced bubble travels from the upstream to the downstream probe. Bubble velocities are obtained from the ratio of the gap between electrodes and the lag time. Bubble length is obtained from the product of bubble velocity and dwell time. In order to avoid improper matching of a signal pair, the following constraints are placed on the matching process. First, the dwell time of each bubble must be within 50 percent relative deviation from the smallest dwell time of the bubble pair. Secondly, the velocity of all bubbles must be greater than the bubble velocity associated with the smaller measured bubble length as calculated from Stokes Law. Finally, all of the measured bubble velocities must be less than the velocity of a bubble slug bridging the column diameter.

In addition to bubble length and velocity information, the signal response can be used to directly obtain gas holdup. The ratio of the total dwell time of bubbles to the total sample time provides the local gas holdup fraction measured by the conductivity probes. The sampling rate for the conductivity probe measurements is 0.5 millisecond per point, and the total sample time for each local measurement is 60 seconds.

Dynamic Surface Tension Model

For a multicomponent liquid mixture, as in slurry phase Fischer-Tropsch reactors, consideration must be given to dynamic surface tension effects on the gas bubble. A depiction of the dynamic surface tension effect is given in Figure 3. The phenomenon is associated with a liquid mixture that contains at least two components with markedly different surface tensions. In this case, the component having the lower surface tension has an excess concentration near the gas bubble film. This excess concentration is a result of the difference in chemical potential between two components with different surface tensions. A dynamic rise in surface tension of an expanding film is realized as a result of the relatively slow migration of molecules of the lower surface tension component into the adsorption layer at the subsurface interface. A depiction of the solute concentration profile for a static and expanding film is shown in Figure 4. The net result of this concentration gradient is to provide an elastic film that enhances the stability of the initial bubble size generated from the distributor plate.

The maximum stabilization of bubble film, or frothing ability, can be estimated from a force and mass balance of the subsurface [7]. For dilute concentrations of a low surface tension liquid component (mole fraction less than 0.1), the maximum frothing ability is obtained from the following equation:

$$x \left(\frac{d\gamma}{dx}\right)^2 = \text{maximum} \qquad (1)$$

Gas Holdup

The gas holdup fractions were visually measured from level differences in the 10.8-cm-diameter and 10-cm-diameter columns for a nitrogen-water system, and the results are shown in Figure 5. This represents a baseline case for a pure component system and demonstrates the effect of the gas distributor. The smaller distributor hole diameter associated with the sintered plate results in a higher gas holdup in the bubble flow regime as compared to the perforated plate distributor. For the bubble column with the sintered plate distributor, slugging flow was observed after reaching a superficial gas velocity of 15 cm/s, and the gas holdup was lower than that obtained at 10 cm/s. At a superficial gas velocity of 20 cm/s, the distributor plate does not have a significant effect on gas holdup.

To test the frothing ability of a surface-active liquid mixture, gas holdup was measured for two different concentrations of aqueous ethanol. The concentrations were chosen from theoretical predictions of frothing ability given by the dynamic surface tension model such that maximum and approximately one-half maximum frothing intensity would be exhibited. In addition, the lower frothing ability mixture had a higher concentration of ethanol than the higher frothing ability mixture so that bulk surface tension effects could be observed. Figure 6 shows the frothing criteria for aqueous ethanol in a bubble column as a function of the mole fraction of ethanol. The maximum theoretical frothing ability occurs at 0.0075 mole fraction ethanol (approximately 1.9 wt. percent), at which the bulk surface tension is 64 dyne/cm. An order of magnitude increase in ethanol concentration to 0.075 mole fraction of ethanol (approximately 19 wt. percent) gives

less than half the frothing ability of the theoretical maximum, and the mixture exhibits a bulk surface tension of 36 dyne/cm.

Figure 7 shows the effect of superficial gas velocity on gas holdup for the 19 weight percent aqueous ethanol—nitrogen system with a sintered plate distributor. A maximum in the gas holdup occurs at a superficial gas velocity between 10 cm/s and 15 cm/s. A marked increase in gas holdup as compared to the pure water system was observed for superficial gas velocities greater than 3 cm/s. Slugging was observed at a superficial gas velocity of 20 cm/s, which is higher than the velocity for slugging with the pure water system.

In Figure 8, the gas holdup is shown as a function of superficial gas velocity for a 1.9 weight percent aqueous ethanol—nitrogen system (near the maximum theoretical frothing ability). The gas holdup increases sharply with increasing gas velocity up to a superficial gas velocity of 10 cm/s and then remains constant up to a superficial gas velocity of 20 cm/s (gas holdup fraction of 90 percent). This remarkable change in the gas holdup fraction with dilute mixtures of aqueous ethanol appears to be qualitatively described by the dynamic surface tension model.

Bubble Measurements

Bubble length and velocity distribution measurements were performed with a twin-probe electrical conductivity device in a slurry bubble column. The slurry phase consisted of a 1.9 weight percent aqueous ethanol solution

and 9 weight percent solids. Nitrogen was employed as the gas phase. The measurements were performed in the 10-cm-diameter column equipped with a 20-micron sintered plate distributor. Interpretation of bubble length and velocity distributions was made with a probability model suggested by Tsutsui and Miyauchi (8). The gamma and log-normal distribution functions were tested as to which function better described the calculated bubble size distribution from the probability model and measured bubble lengths. In all cases, the log-normal distribution was the better representation of the bubble size distributions. The log-normal distribution function for bubble size may be expressed as follows:

$$x\,(d_b) = \exp\left[-(\ln\,(d_b/d_{bg})^2/2\sigma^2\right]/(\sqrt{2\pi}\,\sigma\,d_{bg}) \qquad (2)$$

From this expression, the necessary correlations between bubble length and bubble size distribution parameters have been derived (9):

$$\sigma^2 = \ln\left[8/9\,(S^2(\lambda)/\bar{\lambda}^2 + 1)\right] \qquad (3)$$

and

$$d_{bg} = 1.5\,\bar{\lambda}\exp\left[-2.5\,\sigma^2\right] \qquad (4)$$

The cumulative bubble length distribution can now be expressed in terms of the two log-normal distribution parameters, σ^2 and d_{bg}:

$$CZ(\lambda) = 0.5\ (\lambda/d_{bg})^2\ \exp(-2\sigma^2)\,\mathrm{erfc}\left(\ell n(\lambda/d_{bg})/\sigma\sqrt{2}\right) +$$

$$0.5\ \left\{1 + \mathrm{erf}\left((\ell n(\lambda/d_{bg}) - 2\sigma^2)/\sigma\sqrt{2}\right)\right\} \qquad (5)$$

Calculated values of the cumulative bubble length distribution have been compared with measured values obtained from the conductivity probe measurements in a slurry bubble column. An example of the agreement between calculated and measured bubble distributions is given in Figure 9. The slurry consisted of 9 weight percent solids in a 1.9 weight percent aqueous ethanol solution. The superficial gas velocity was 2.22 cm/s, which was the critical gas velocity required for complete suspension of solids. The radial position of the conductivity probe was halfway between the center and wall of the column (r^*=0.5), and the axial position of the probe was at 179 cm (Z^*=0.60). Good agreement is achieved between the calculated and measured cumulative bubble length distribution. The calculated bubble length distribution indicates that 50 percent of the buboles have a diameter less than 2 mm.

The cumulative bubble size distribution may be expressed as follows:

$$CX(d_b) = 0.5 + 0.5\ \mathrm{erf}\left(\ln(d_b/d_{bg})/\sigma\sqrt{2}\right) \qquad (6)$$

The Sauter mean bubble size is only a function of the average bubble length:

$$d_{vs} = 1.5\ \bar{\lambda} \qquad (7)$$

The interfacial area of gas is a function of the gas holdup and Sauter mean bubble size:

$$a = 6\ \varepsilon_g / d_{vs} \qquad (8)$$

For the conditions given in Figure 9, the Sauter mean bubble size was 0.364 cm, and the interfacial area was 1.71 cm^{-1}. The bubble size and gas holdup did not vary significantly with radial position. The average gas holdup was 10 percent, and the average Sauter mean bubble size was 0.360 cm.

Local gas phase characteristic measurements were also made at 71 cm and 289 cm from the distributor plate. For the measurements near the top of the bubble column (Z^*=0.97), no significant change was observed in the bubble size and gas holdup as compared to measurement at Z^* of 0.60. However at Z^* of 0.24, the gas holdup was reduced to 6 percent, and the Sauter mean bubble size increased to 0.417 cm. Consequently, the interfacial area was reduced by 45 percent as compared to the interfacial area measurements at Z^* of 0.60 and 0.97. A possible explanation of this reduction in interfacial area involves the axial solids concentration distribution. At Z^* of 0.24, the solids concentration in the slurry was 2 weight percent; but at Z^* of 0.60, it was reduced to 0.5 weight percent; and at Z^* of 0.97, it was further reduced to 0.2 weight percent. It has been reported previously (5) that the gas holdup decreases with an increase in solids concentration.

In addition to the bubble size distribution measurements, the bubble velocity distribution was obtained as a function of measured bubble length and the calculated bubble size distribution. For small bubbles, the

velocity of a single bubble is proportional to the bubble size, and for large bubbles, it is proportional to the square root of the bubble size. As a first approximation, the bubble velocity was assumed to be a linear function of bubble size:

$$U_b = p + q\, d_b \tag{9}$$

The average velocity is related to the mean bubble size:

$$\bar{U}_b = p + q\, \bar{d}_b \tag{10}$$

Hess (9) has derived an expression for the bubble velocity as a function of measured bubble length from the assumption given in Equation (9):

$$U_b = p + q\, d_{bg}\, \mathrm{erfc}\left((\ln(\lambda/d_{bg}) - \sigma^2)/\sigma\sqrt{2}\right)/\mathrm{erfc}\left(\ln(\lambda/d_{bg})/\sigma\sqrt{2}\right) \tag{11}$$

Figure 10 gives the bubble velocity distribution as a function of measured bubble length obtained in a nitrogen--aqueous ethanol--glass beads system. The solids concentration in the slurry was 9 weight percent, and the ethanol concentration in water was 1.9 weight percent. The superficial gas velocity was 2.22 cm/s. These are the same conditions employed in the bubble size distribution measurements. The bubble velocity initially increases linearly with bubble length for small bubbles. For lengths greater than 0.15 cm, the velocity may increase at a reduced rate, but the data have considerable scatter. The calculated bubble velocity distribution predicts the measured bubble velocity reasonably well above a bubble length

of 0.15 cm but fails below a bubble length of 0.1 cm. This indicates a need for assuming a different expression for the bubble velocity distribution as a function of bubble size.

Figure 11 shows the calculated bubble velocity as a function of bubble size for the same conditions given in Figure 10. The mean bubble velocity as calculated from Equation (10) is 18.7 cm/s. The ratio of the superficial gas velocity to the mean bubble velocity should indicate the gas holdup fraction if the bubbles are rising vertically through the column. This ratio is 0.119 as compared to a locally measured gas holdup of 0.103. Some of the difference between these two values may be attributed to the over-prediction of bubble velocity for the small bubbles.

Discussion

The results of the bubble measurements given in the preceding sections indicate the need to properly understand the physical and chemical composition of the liquid phase in a slurry bubble column in order to predict the bubble dynamics. In addition, the effect of the solid phase and the initial bubble size generated from a gas distributor must be considered. The prediction of gas holdup and bubble size from the bulk transport properties of the liquid phase appears to be possible for liquids that do not contain a "surface-active" component. Gas holdup appears to be directly related to the superficial gas velocity and mean bubble size when operating in the bubble flow regime. The gas interfacial area is a function of the superficial gas velocity, mean bubble size, and Sauter mean bubble size. Further

experimental investigation of bubble dynamics for hot, pressurized slurry waxes similar to the slurry phase expected in a Fischer-Tropsch reactor is needed to ascertain the effect of a variable-composition organic mixture on the hydrodynamics and, in particular, to determine the effect of any "surface-active" components that may be present. According to the dynamic surface tension model, the dynamic surface tension effect becomes important for a two-component liquid mixture if the frothing criteria expressed in Equation (1) exceeds 1000 $dyne^2/cm^2$.

For proper scale-up of a slurry bubble column reactor, the diameter and length of the column should be sufficient to avoid wall effects on gas holdup and flow regime. The flow regime map given by Deckwer et al. [10] indicates the influence of column diameter on the flow regime transitions. For column diameters greater than 10 to 15 cm, the flow regime transitions appear to be independent of superficial gas velocity and column diameter. This corresponds to the column diameter effect on gas holdup given by Hughmark [11], in which the gas holdup is a function of column diameter for diameters less than 10 cm. This has been confirmed independently for a perforated plate distributor at our laboratory for column diameters between 2.22 cm and 10.8 cm. For this range of column diameters, the gas holdup was proportional to the Froude number ($\overline{U}_g^2/gD$) to the 1/3 power in the bubble flow regime and had a correlation coefficient of 0.98.

Conclusions

An experimental technique and subsequent analysis have been developed to determine the bubble size and velocity distributions in a slurry bubble column cold model. Dynamic surface tension effects have been observed for a two-component liquid mixture. The maximum frothing ability of a "surface-active" species qualitatively agrees with a dynamic surface tension model. Increased gas holdup and interfacial area are observed with the addition of a "surface-active" component. In addition, increased gas holdup and interfacial area are observed with a sintered plate compared to a perforated plate. The presence of solids reduces the gas holdup and increases the bubble size.

Acknowledgments

The authors are grateful to Donn Smith and Charles Brodd for performing the bubble dynamic experiments and constructing the slurry bubble column apparatus. We also thank Robert James for photography that confirmed the proper design of the conductivity probes.

Disclaimer

Nomenclature

a	–	gas interfacial area per unit volume of column, cm^{-1}
$CX(d_b)$	–	cumulative bubble size distribution
$CZ(\lambda)$	–	cumulative bubble length distribution
d_b	–	bubble size, cm
d_{bg}	–	geometric mean bubble size, cm
d_{vs}	–	Sauter mean bubble size, cm
D	–	column diameter, cm
g	–	gravitational acceleration, cm/s^2
p	–	bubble velocity parameter, cm/s
q	–	bubble velocity parameter, s^{-1}
r^*	–	dimensionless radial position
$S^2(\lambda)$	–	variance of bubble length, cm^2
U_b	–	bubble velocity, cm/s
$\overline{U}_b$	–	mean bubble velocity, cm/s
$\overline{U}_g$	–	superficial gas velocity, cm/s
X	–	mole fraction of low surface tension component in liquid
$X(d_b)$	–	frequency distribution of bubble size
Z^*	–	dimensionless axial position

Greek Symbols

γ	–	surface tension of liquid, dyne/cm
ϵ_g	–	gas holdup
λ	–	bubble length, cm
$\overline{\lambda}$	–	mean bubble length, cm
σ^2	–	variance of bubble size

References

(1) Deckwer, W.-D., Serpemen, Y., Ralek, M., and Schmidt, B., "On the Relevance of Mass Transfer Limitations in the Fischer-Tropsch Slurry Process," Chem. Eng. Sci., 36, 765-771, 1981.

(2) Satterfield, C.N., and Huff, G.A., "Mass Transfer Limitations in Fischer-Tropsch Slurry Reactors," Chem. Eng. Sci., 36, 790-791, 1981.

(3) Deckwer, W.-D., Serpemen, Y., Ralek, M., and Schmidt, B., "Response to Letter of Satterfield and Huff Concerning Mass Transfer Limitations in Fischer-Tropsch Slurry Reactors," Chem. Eng. Sci., 36, 791-792, 1981.

(4) Kuo, J.C.W., "Slurry Fischer-Tropsch/Mobil Two-Stage Process of Converting Syngas To High Octane Gasoline," Final Report DOE/PC/30022 - 10, June, 1983.

(5) Smith, D.N., Fuchs, W., Lynn, R.J., Smith, D.H., and Hess, M., "Bubble Behavior in a Slurry Column Reactor Model," 185th ACS National Meeting, Industrial and Engineering Chemistry Division, Seattle, Washington, March, 1983.

(6) Fuchs, W., and Smith, D.N., "Conductivity Probe and Data Acquisition for a Liquefaction Cold Model," Proceedings of the 1982 Symposium on Instrumentation and Control for Fossil Energy Processes, ANL-82-62, 233-246, June 7-9, 1982.

(7) Andrew, S.P.S., "Frothing in Two-Component Liquid Mixtures," International Symposium on Distillation, Instn. Chem. Engrs., 73-78, 1960.

(8) Tsutsui, T., and Miyauchi, T., "Fluidity of a Fluidized Catalyst Bed and Its Effect on the Behavior of the Bubbles," Int. Chem. Eng., 20, 386-393, 1980.

(9) Hess, M., "Alternate Distribution Functions of Bubble Diameters Log-Normal and Log-Gamma Distribution Functions," Final Report DE-AP22-83PC10614, July, 1983.

(10) Deckwer, W.-D., Louisi, Y., Zaidi, A., and Ralek, M., "Hydrodynamic Properties of the Fischer-Tropsch Slurry Process," Ind. Eng. Chem., Process Des. Dev., 19, 699-708, 1980.

(11) Hughmark, G.A., "Holdup and Mass Transfer in Bubble Columns," Ind. Eng. Chem., Process Des. Dev., 6, 218-220, 1967.

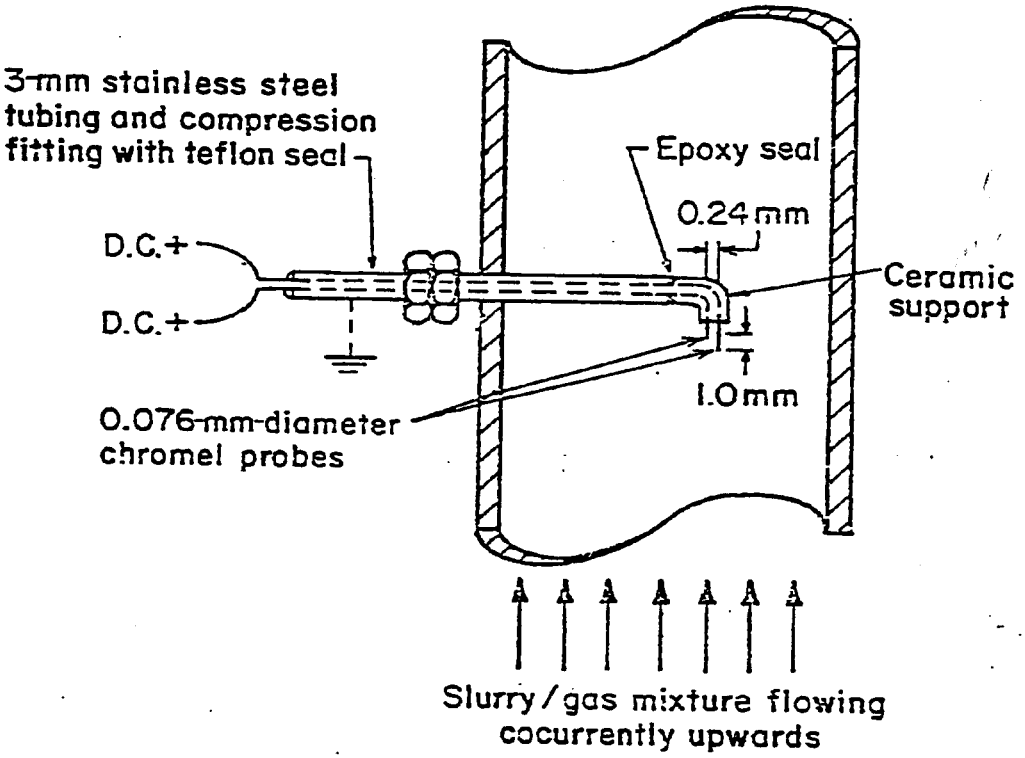

Figure 1- Probe configuration for conductivity measurements in 10.8-cm-i.d. slurry bubble column apparatus.

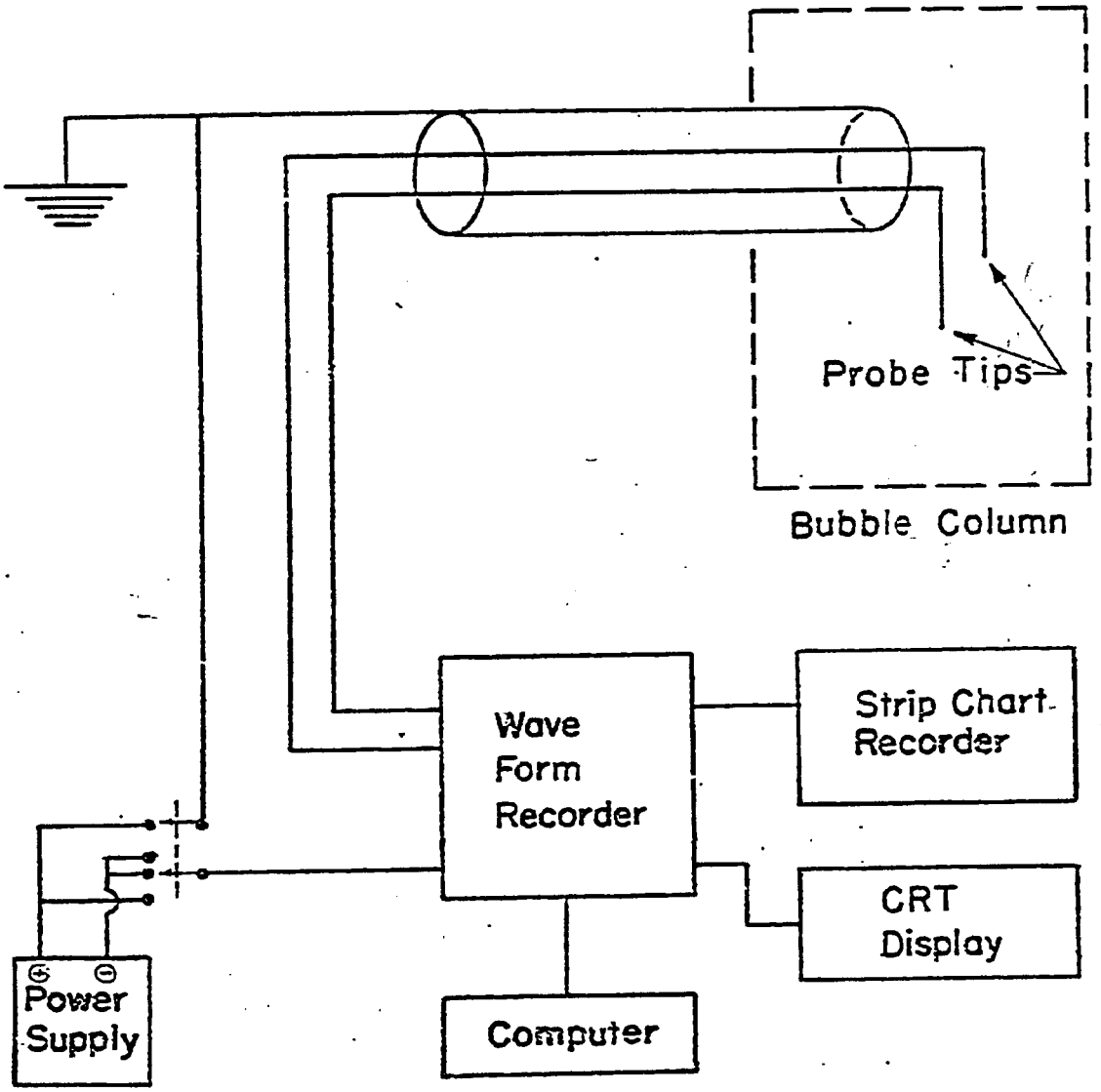

Figure 2- Two-point electrical conductivity probe circuit and data acquisition system.

L-82753

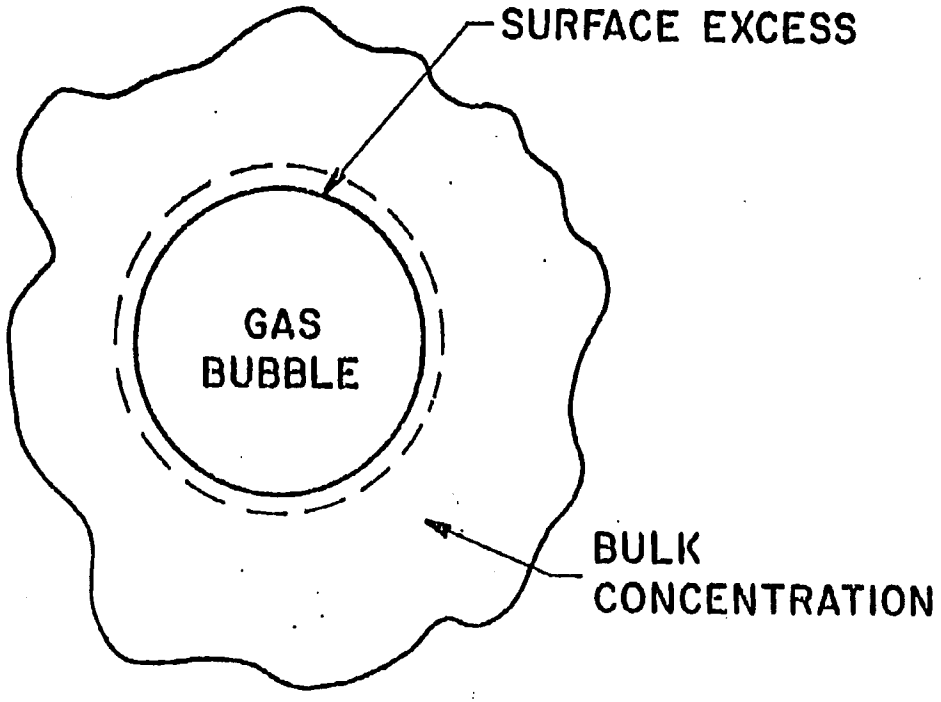

Figure 3-Dynamic surface tension model.

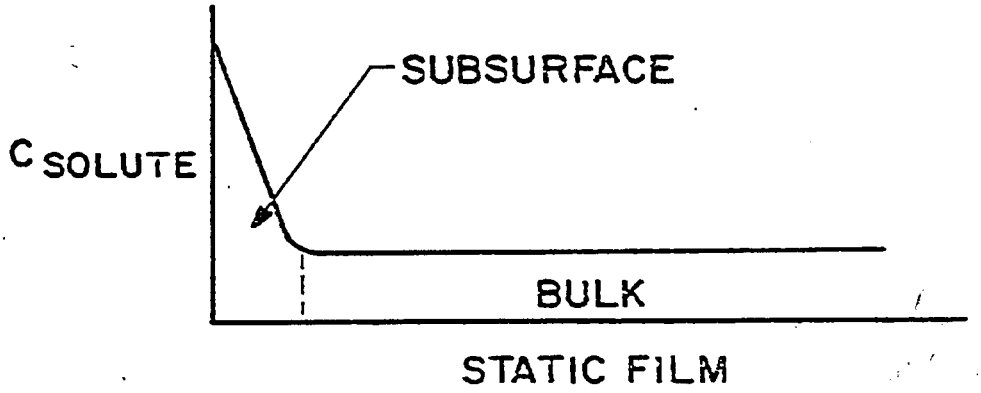

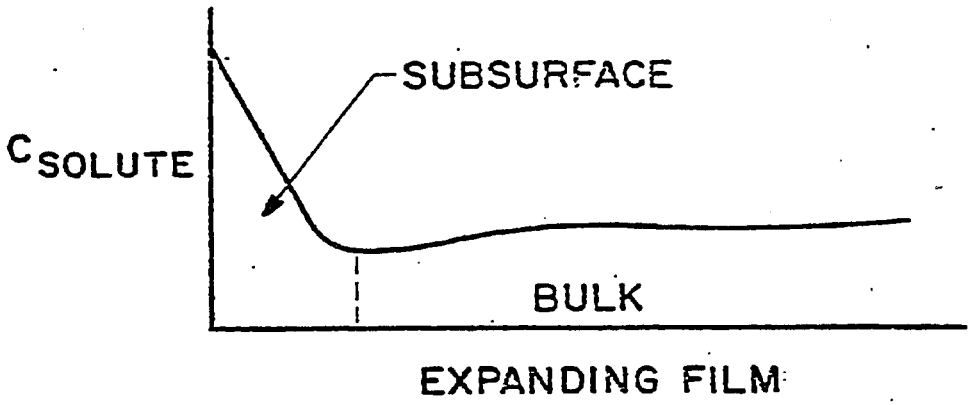

Figure 4- Solute concentration profile for dynamic surface tension model.

BSI/4228

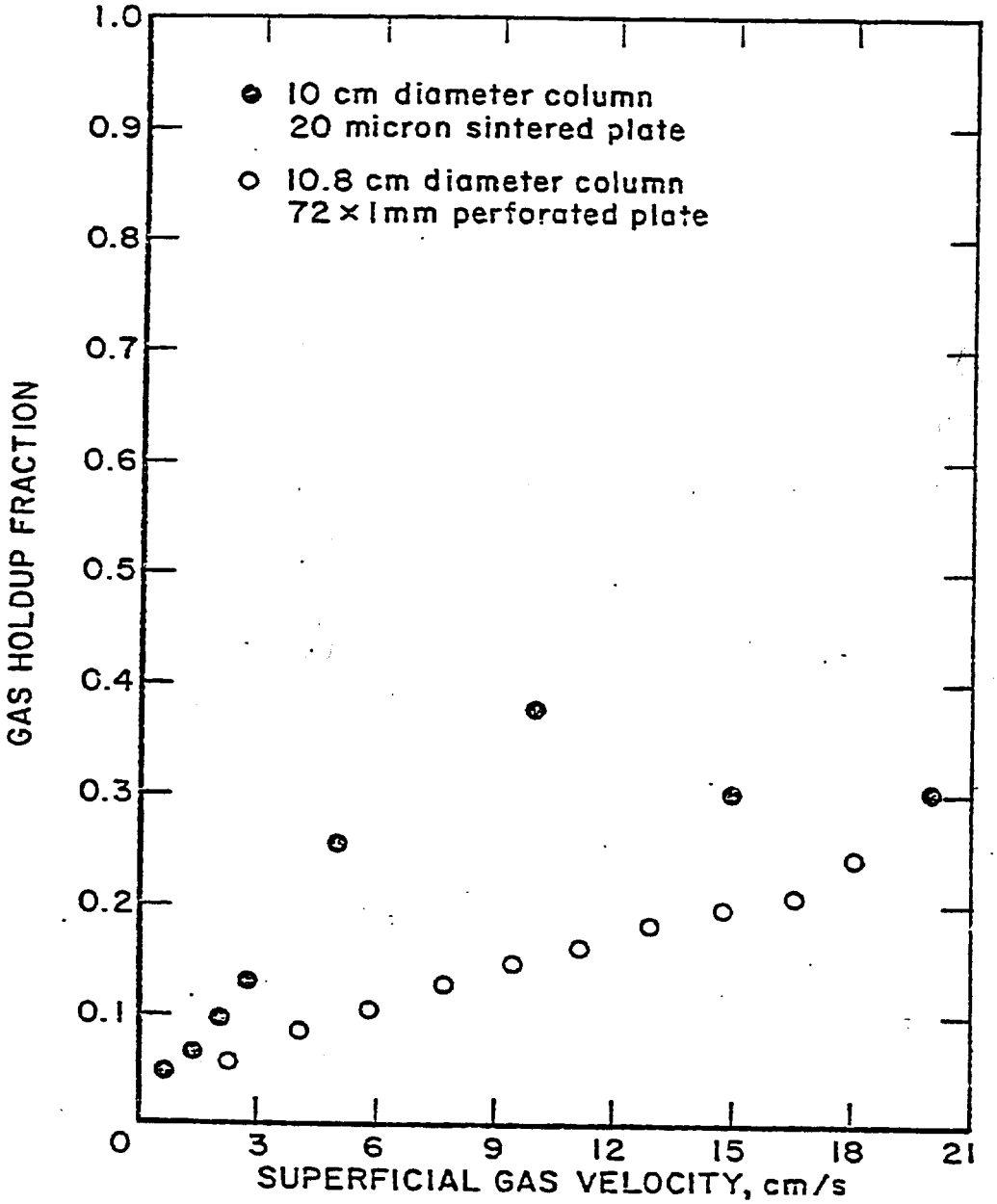

Figure 5 - Gas holdup as a function of superficial gas velocity for a nitrogen-water system.

BSW4231

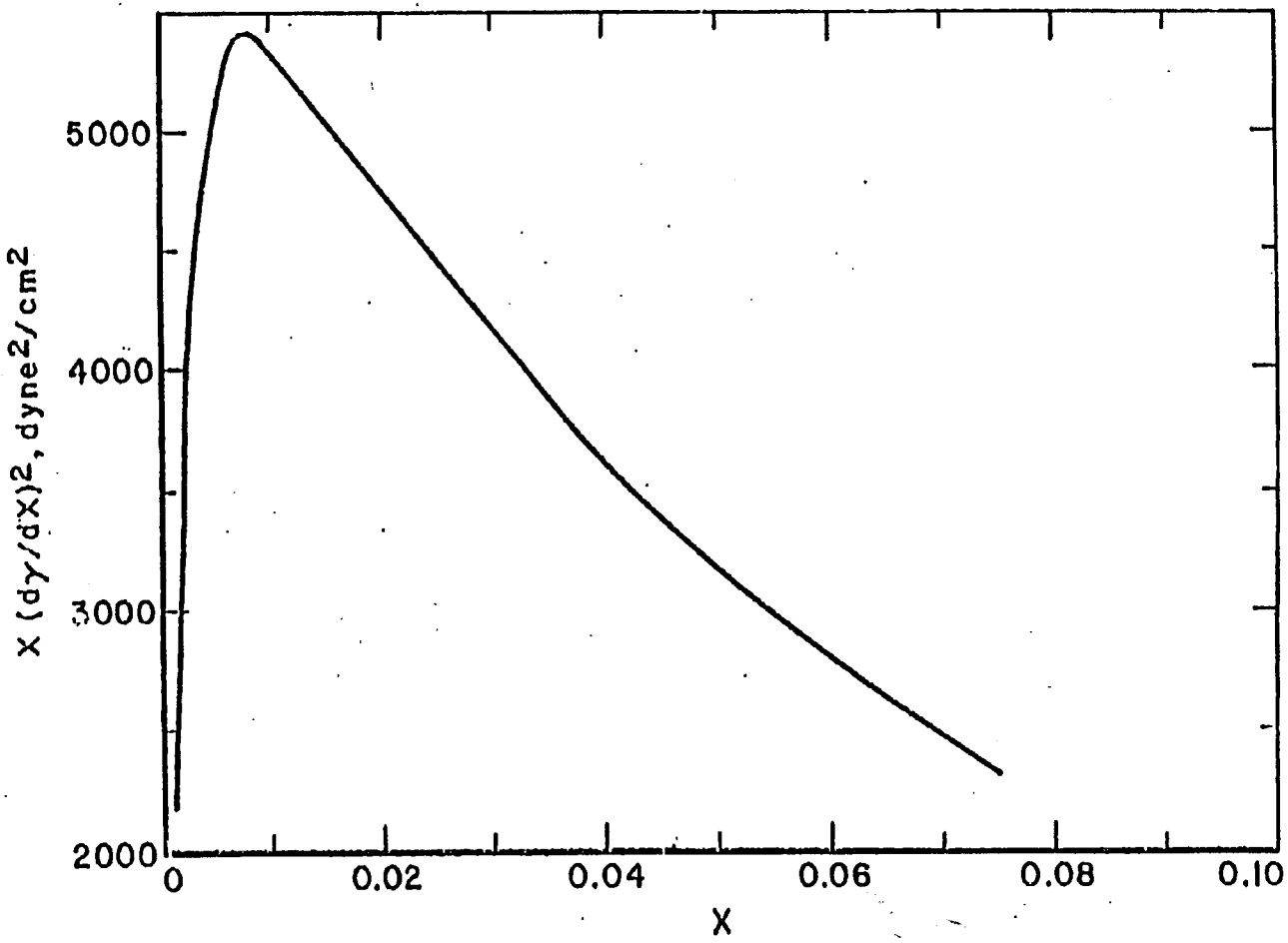

Figure 6· Frothing criteria for aqueous ethanol mixture in bubble column.

OSM4180

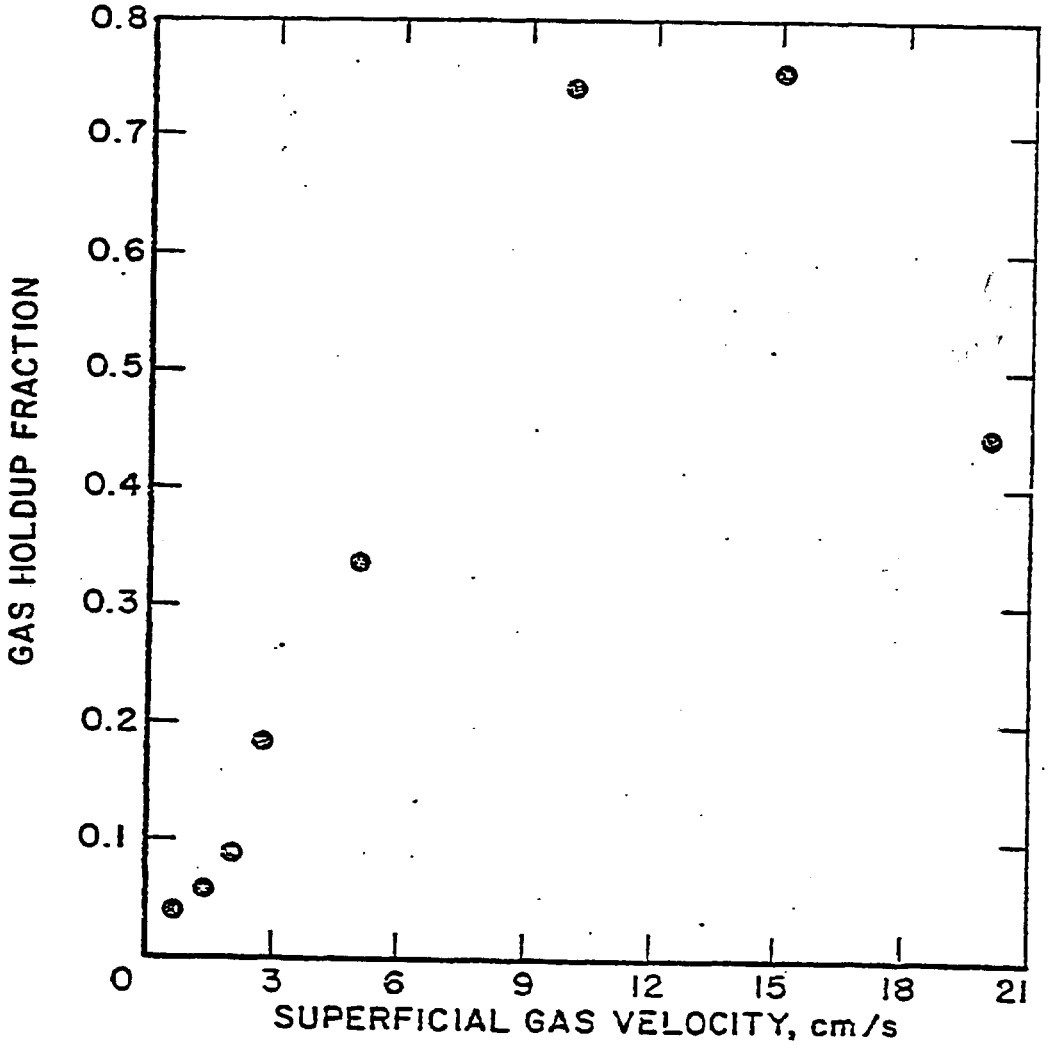

Figure 7-Gas holdup as a function of superficial gas velocity for nitrogen and 19 wt. percent aqueous ethanol system.

BSI/4230

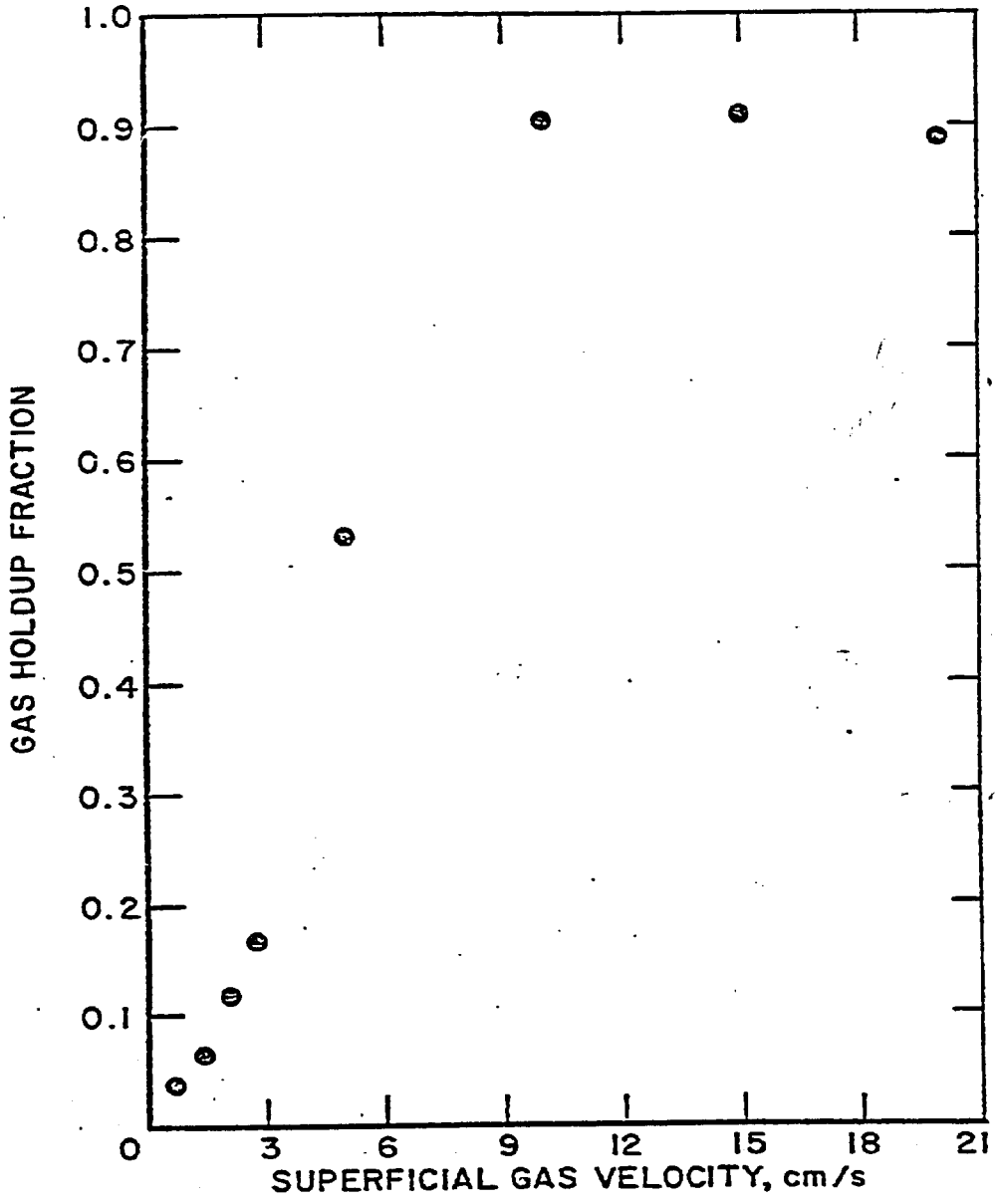

Figure 8- Gas holdup as a function of superficial gas velocity for nitrogen and 1.9 wt. percent aqueous ethanol system.

BSU4185

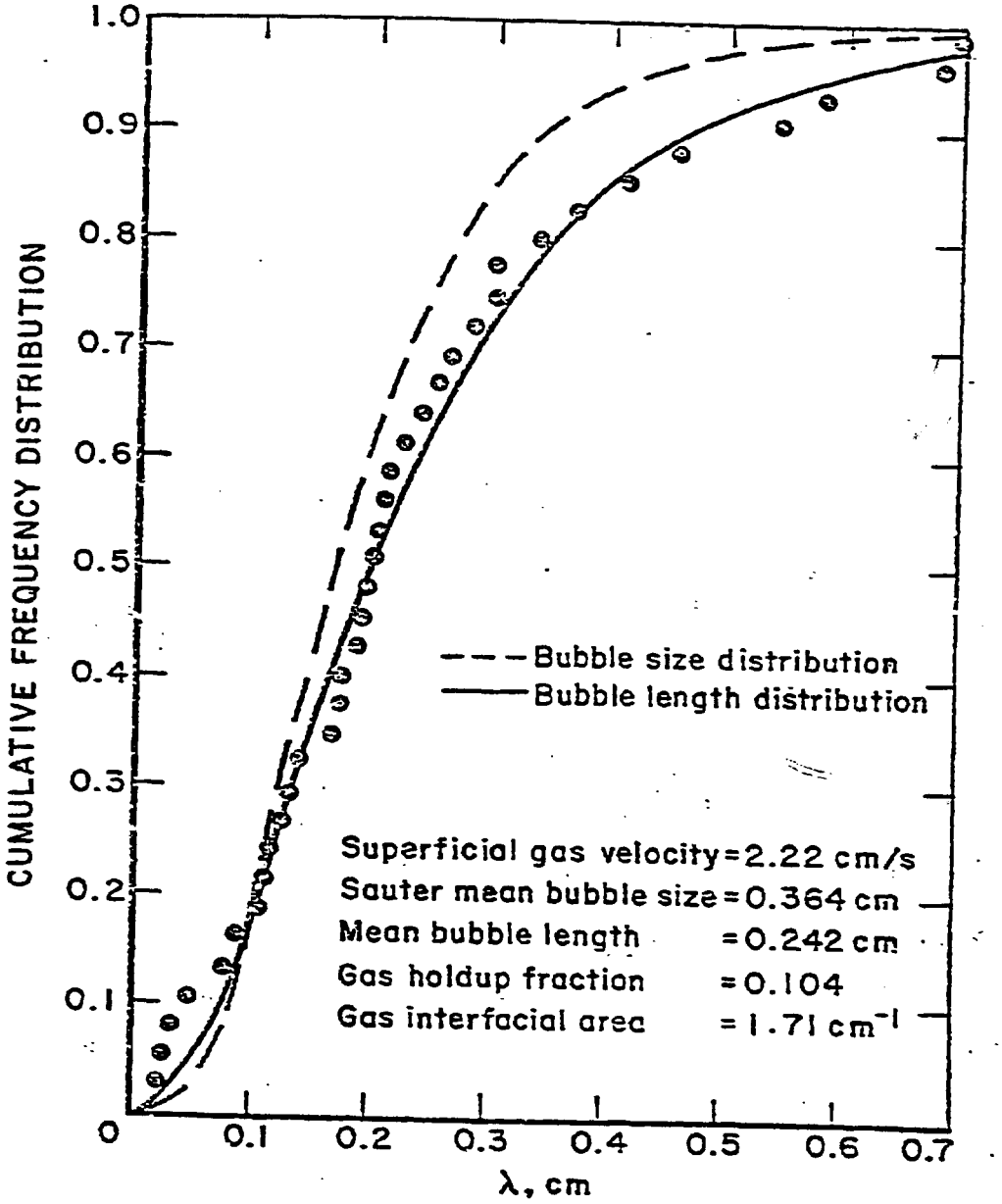

Figure 9- Comparison of experimental and calculated cumulative frequency distributions of bubbles (1.9 wt. percent aqueous ethanol, $Z^* = 0.60$, $r^* = 0.5$)

BSU4186

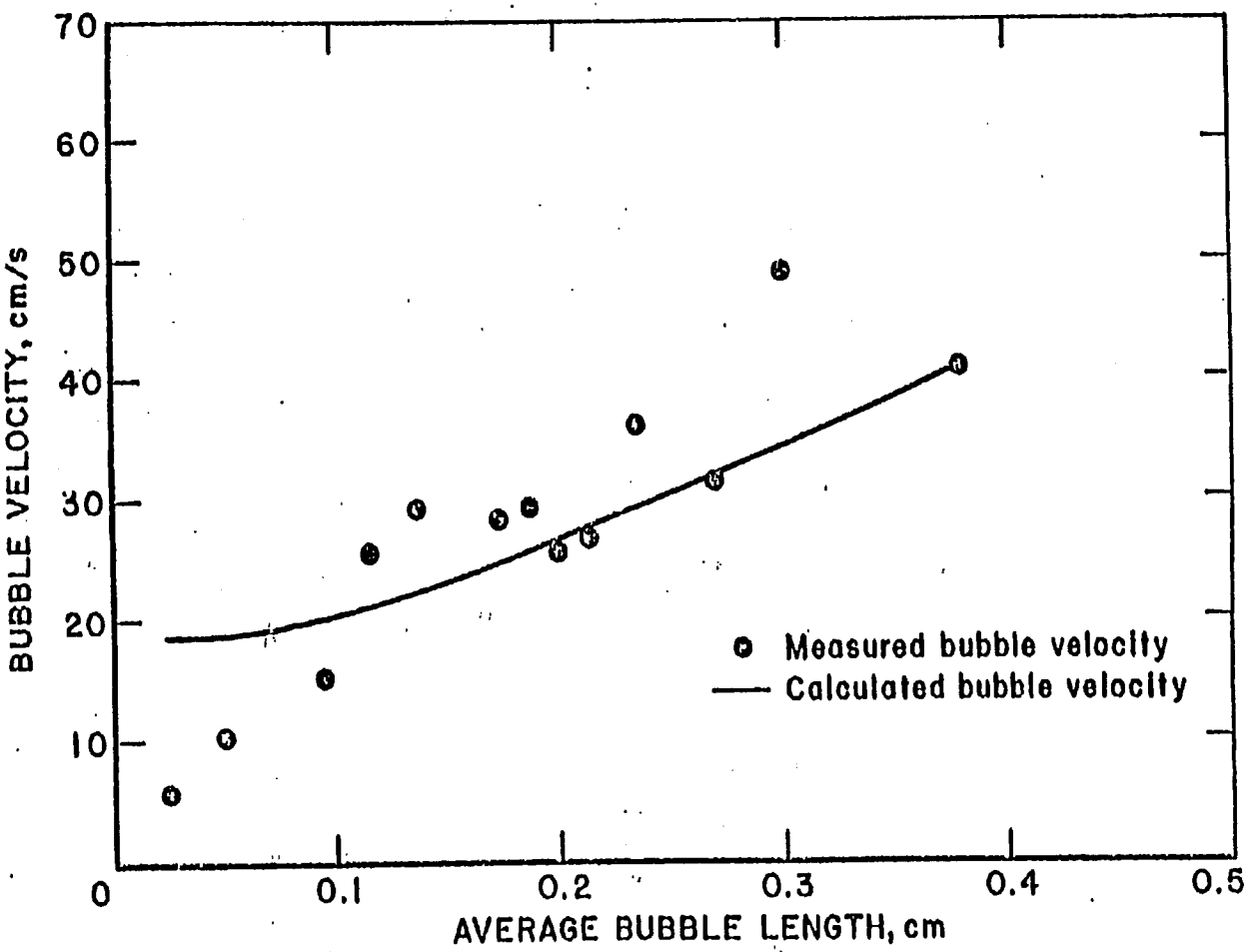

Figure 10. Bubble velocity as a function of measured bubble length (superficial gas velocity is 2.22 cm/s for 1.9 wt. percent aqueous ethanol system).

BSU4179

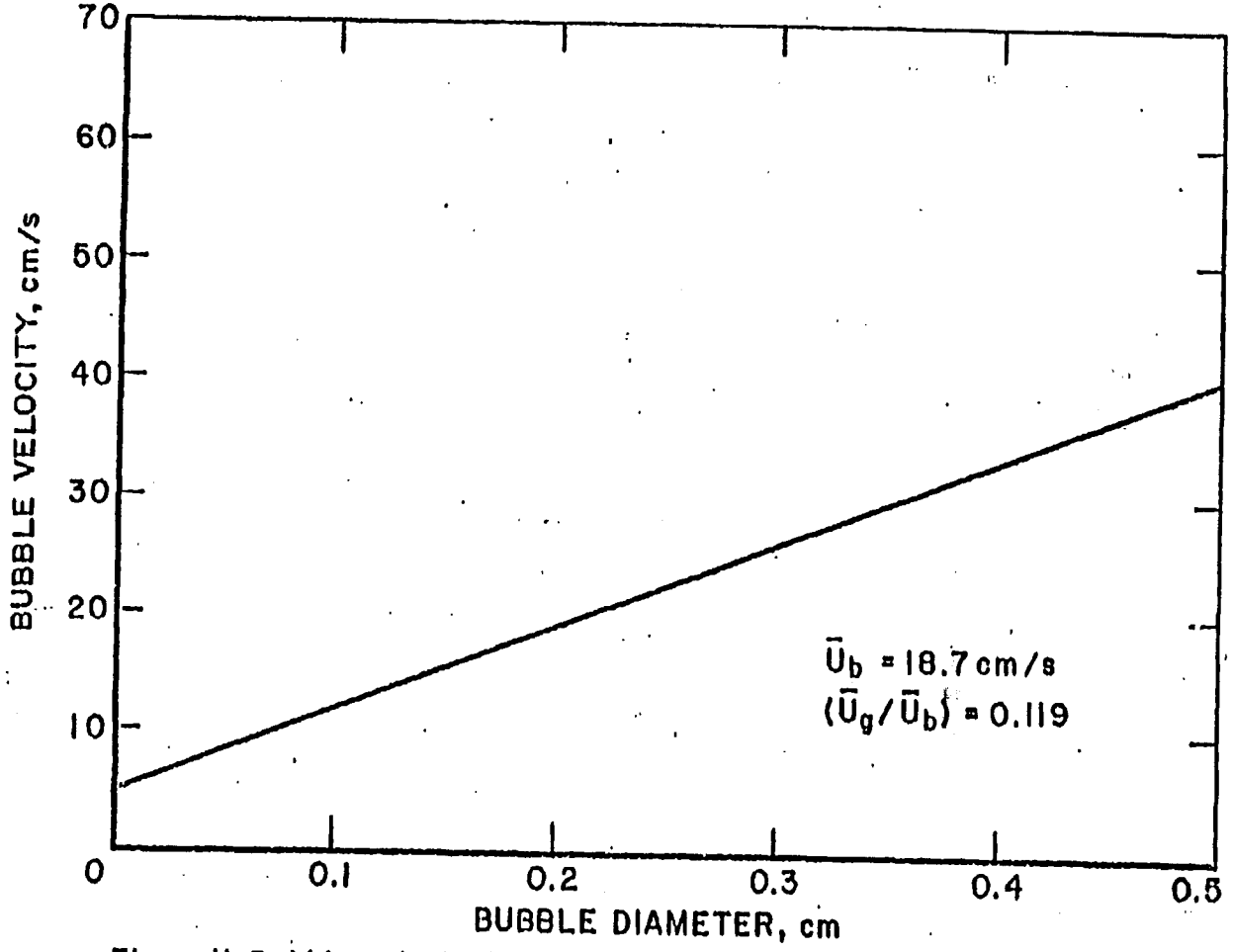

Figure 11- Bubble velocity as function of bubble size (superficial gas velocity is 2.22 cm/s in 1.9 wt percent aqueous ethanol system).

BSI/4178